# BEAM BASED MEASUREMENTS WITH SUPERCONDUCTING WIGGLERS AT THE CANADIAN LIGHT SOURCE WITH APPLICATIONS TO NONLINEAR BEAM DYNAMICS

W. A. Wurtz*, L. O. Dallin, and M. J. Sigrist,
Canadian Light Source, Saskatoon, Saskatchewan, Canada

*Abstract*

The Canadian Light Source employs two superconducting wigglers for the production of hard x-rays. These wigglers cause a large decrease in injection efficiency. While such a decrease is not unexpected due to the large distortion to the linear optics, a correction to the linear optics does not restore injection efficiency. This inability to restore injection is not predicted by a kickmap model of the wiggler. We performed beam based measurements to construct a phenomenological, nonlinear model of the wiggler. Particle tracking with this wiggler model shows that the reduction in dynamic aperture is due to the amplitude dependent tune shift crossing a resonance, even with the linear optics corrected. Moving the tunes allows us to avoid this resonance and measurements at these tunes show that injection efficiency is not greatly affected by the wigglers.

## INTRODUCTION

The Canadian Light Source (CLS) employs two superconducting wigglers (SCW) produced by the Budker Institute of Nuclear Physics (BINP). The Biomedical Imaging and Therapy (BMIT) and Hard X-ray MicroAnalysis (HXMA) beamlines use SCWs with peak fields 4.3 T and 2.1 T respectively [1, 2]. They have a detrimental effect on injection efficiency for the nominal tunes (10.22, 4.32). SCW2.1 reduces injection efficiency a few percent while SCW4.3 can reduce it from the nominal $\sim 60\%$ to $\sim 3\%$ under some conditions.

Figure 1 shows a beam position monitor (BPM) sum measurement, which functions as a rough turn-by-turn current monitor, with and without SCW4.3. For this measurement, a single shot was injected into an empty storage ring. Notice how the wiggler causes current to be lost over several hundred turns.

It is not surprising that that these wigglers have a detrimental effect on injection efficiency due to their large perturbation on the linear optics. However, we are not able to restore injection when we correct the linear optics. This is in contrast to the results of Diamond Light Source, which has two similar BINP wigglers, including a 4.2 T model. Diamond reports a restoration of injection efficiency after correcting the linear optics [3]. Since the reduction in injection efficiency is not due to linear optics, we must now consider nonlinear optics.

The first non-linear effect to consider is dynamic focusing due to field roll-off [4]. However, when we model the wigglers using RADIA [5], we do not find sufficient field roll-off to explain the injection losses [6]. Kickmaps [7] produced from the RADIA model do not predict the loss of dynamic aperture. The poles of the wigglers appear to be sufficiently wide to make field roll-off effects negligible.

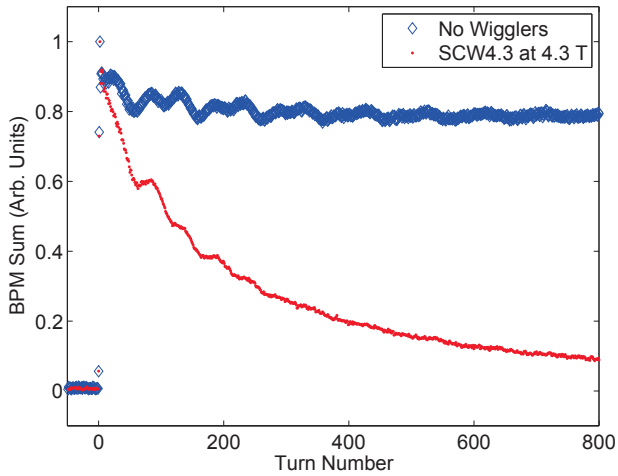


Figure 1: Turn-by-turn current measurement from a BPM sum with and without SCW4.3.

In order to understand the source of the reduction in injection efficiency, we perform measurements to construct a phenomenological, nonlinear model.

## MEASUREMENTS

We have measured the tune shift and beta beat due to SCW4.3. These measurements agree well with the simulation, with the lone exception of a horizontal tune shift of $-0.0014 \pm 0.0002$, which does not agree with the kickmap prediction [6]. We look to beam-based measurements of higher order multipoles to explain the reduction in injection efficiency.

Since the CLS storage ring operates with dispersion in the straight sections, we can move the stored beam horizontally by changing the beam energy. We define the fractional momentum shift

$$\delta \equiv \frac{p - p_0}{p_0} \quad (1)$$

where $p_0$ is the reference momentum ($\sim$ 2.9 GeV/c for CLS) and $p$ is the actual momentum of the beam. The hor-

* ward.wurtz@lightsource.ca


ISBN 978-3-95450-115-1

izontal tune can be written as a function of $\delta$

$$\nu_x(\delta) = \nu_{x,0} + \chi_x^{(1)}\delta + \chi_x^{(2)}\delta^2 + \chi_x^{(3)}\delta^3 + \dots \quad (2)$$

and similarly for the vertical. In this expansion $\nu_{x,0}$ is the on-momentum tune and $\chi_x^{(1)} = \frac{d\nu_x}{d\delta}\big|_0$ is the chromaticity, which we will refer to as the first-order chromaticity. As the momentum deviation becomes larger, we will consider chromaticities of higher order and will refer to $\chi_x^{(2)}$ as the second order chromaticity, etc.

The rf frequency at CLS is approximately 500 MHz. We control the beam energy by varying this frequency and measure the horizontal and vertical tunes at a variety of frequencies. We perform the measurement with a bare lattice and with SCW4.3 at maximum field. By fitting equation (2) to the data, we are able to extract $\nu_x$, $\chi_x^{(1)}$, $\chi_x^{(2)}$, and $\chi_x^{(3)}$, and similar for the vertical. Differences in these quantities with and without the wiggler tells us about the the low order multipole structure of the wiggler

Figures 2 and 3 show a sample measurement for the bare lattice configuration. By fitting the expansion from equation (2), we are able to determine the four coefficients.

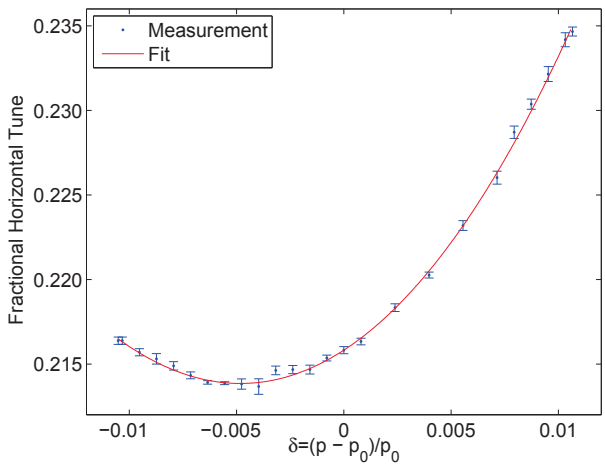


Figure 2: Measurement of fraction horizontal tune at various beam energies.

By carefully estimating and propagating uncertainties, we determine that there are shifts in both $\chi_x^{(1)}$ and $\chi_x^{(2)}$. The shifts in $\chi_z^{(1)}$ and $\chi_z^{(2)}$ as well as the third-order chromaticities are within uncertainty bounds of zero. The measured shifts in tune and chromaticity are reported in Table 1.

Table 1: Measured shifts in horizontal (H) and vertical (V) tunes and chromaticities due to SCW4.3

| | $\Delta\nu$ | $\Delta\chi^{(1)}$ | $\Delta\chi^{(2)}$ |
|---|---|---|---|
| H | -0.0014 ± 0.0002 | -0.083 ± 0.015 | -3.4 ± 1.8 |
| V | 0.0146 ± 0.0002 | -0.010 ± 0.017 | 4.5 ± 5.4 |

In order to compare the measurement with simulation, we use the optics code elegant [8]. The vertical tune

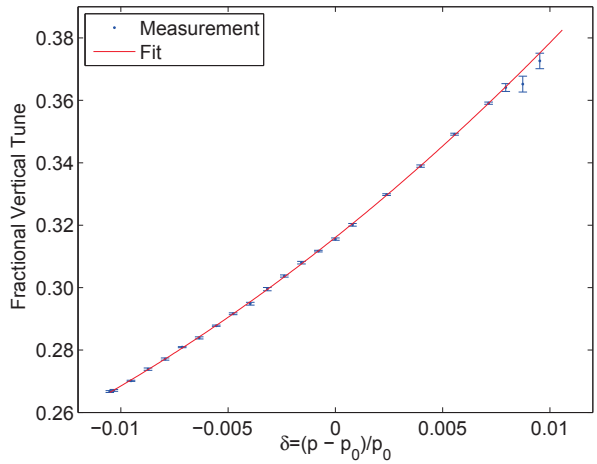


Figure 3: Measurement of fraction vertical tune at various beam energies.

shift agrees well with the value of 0.0149 predicted by the kickmap and the value of 0.0147 predicted by the CWIGGLER [9, 10] element of elegant. No shifts in $\nu_{x,0}$, $\chi_x^{(1)}$ or $\chi_x^{(2)}$ are predicted by the simulation.

By symmetry, we expect field roll-off to generate only terms that look like odd multipoles [4]. Field roll-off could explain the shifts in $\nu_{x,0}$ and $\chi_x^{(2)}$, but not the shift in first-order chromaticity, $\chi_x^{(1)}$. While the source of these multipoles is not clear, we speculate that they may be due to variations in the field integrals, not dynamic effects. This is supported by simulations which show that we can generate integrated multipoles of these orders by misalignments and imperfections in the wiggler geometry [6].

## MODELING

In order to include the measured tune and chromaticity shifts in our simulation, we add several thin lenses to the center of our wiggler models. In order to account for the anomalous horizontal tune shift, we add a matrix that is the identity matrix with an addition element, $R_{21}$ ($R_{43}$ remains zero). The strengths of these elements are given in Table 2. The measurement has provided values for three low order multipoles with uncertainty bounds. We plan to use local orbit bumps and experimental frequency map analysis to further study the effects of SCW4.3 and to determine values for higher order multipoles.

Table 2: Integrated multipoles of SCW4.3 calculated from the measured tune and chromaticity shifts

| Integrated Multipole | Kick Units (Powers of m) | Magnetic Field Units (T and m) |
|---|---|---|
| $R_{21}$ | $0.0019 \pm 0.0003\ \mathrm{m}^{-1}$ | $0.018 \pm 0.003$ T |
| $K_2L$ | $-0.70 \pm 0.12\ \mathrm{m}^{-2}$ | $-6.8 \pm 1.2$ T/m |
| $K_3L$ | $-430 \pm 160\ \mathrm{m}^{-3}$ | $-4200 \pm 1500$ T/m$^2$ |

We can now use our phenomenological, nonlinear model in a simulation to study the effects of SCW4.3 on dynamic aperture. Figure 4 shows the calculated frequency map [11] for an ideal model of the bare lattice. We add our phe-

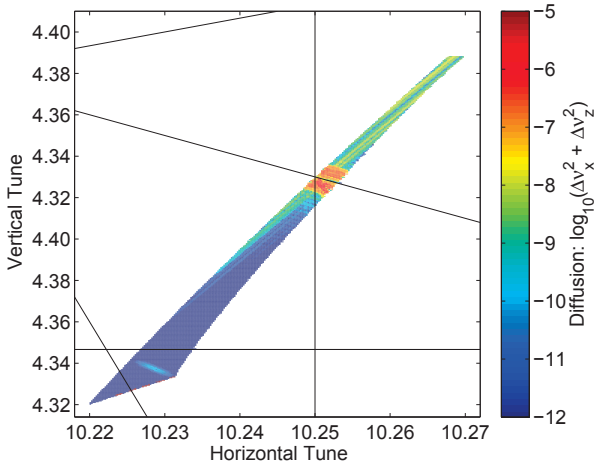


Figure 4: Frequency map for the bare lattice.

nomenological, non-linear model of SCW4.3 to the simulation and obtain the frequency map shown in Figure 5. In

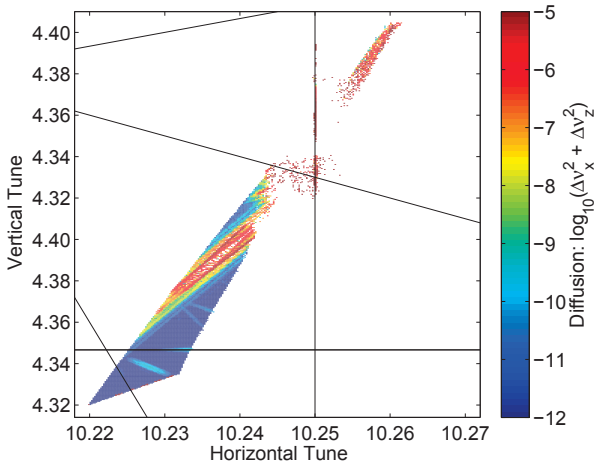


Figure 5: Frequency map with the phenomenological, nonlinear model of SCW4.3.

Figure 5, the $\nu_x + 2\nu_z = 1$ sextupole resonance severs the frequency map, which is not observed with the kickmap model. The wiggler causes a large loss of dynamic aperture for beams with oscillation amplitudes similar to the injected beam.

The reduction in dynamic aperture can be avoided by moving the operating point further from the $\nu_x + 2\nu_z = 1$ resonance. Figure 6 shows dynamic aperture for nearby operating points. We have experimentally verified that the wiggler does not cause additional injection losses when we use tunes (10.20, 4.27).

In order to explain the reduction in dynamic aperture due to the SCWs, we constructed a phenomenological, nonlin-

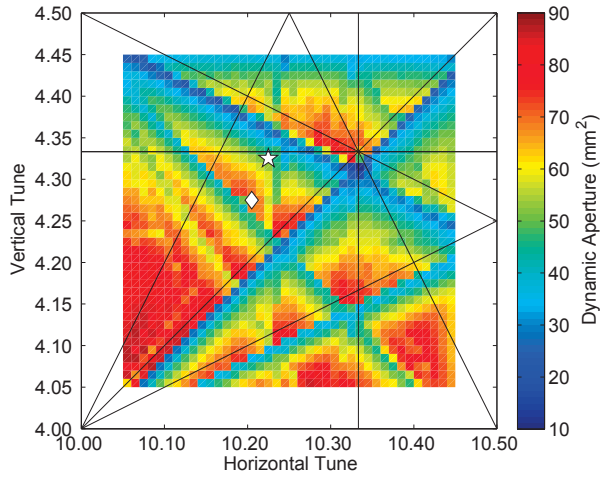


Figure 6: Dynamic aperture with SCW4.3; the nominal tunes (10.22, 4.32) are marked with a star and an alternate operating point (10.20, 4.27) is marked with a diamond.

ear model of the wigglers created from beam-based measurements. We then used this model to determine that the reduction in dynamic aperture is due to the amplitude dependent tune shift crossing a resonance. Changing the tunes allows us to avoid this resonance and restore injection efficiency. While will concentrated on SCW4.3, the discussion also applies to SCW2.1.

## ACKNOWLEDGMENT

We would like to thank C. Steier and the staff of the Advanced Light Source for their assistance with frequency map analysis. We would also like to thank the staff of Diamond Light Source for their helpful discussions on superconducting wigglers. This research was enabled by the use of computing resources provided by WestGrid and Compute/Calcul Canada.

## REFERENCES

[1] S.V. Khruschev *et al.*, Nucl. Instr. and Meth A 603, 7 (2009).
[2] S.V. Khruschev *et al.*, Nucl. Instr. and Meth A 575, 38 (2007).
[3] B. Singh *et al.*, "Beam dynamics effect of insertion devices at Diamond storage ring", IPAC10 (2010).
[4] J. Safranek *et al.*, Phys. Rev. ST AB 5, 010701 (2002).
[5] P. Elleaume, O. Chubar and J. Chavanne, "Computing 3D magnetic fields from insertion devices", PAC97 (1997).
[6] C. Baribeau *et al.*, These Proceedings (2012).
[7] P. Elleaume, "A new approach to the electron beam dynamics in undulators and wigglers", EPAC92 (1992).
[8] M. Borland, "elegant: A flexible SDDS-compliant code for accelerator simulation", LS-287 (2000).
[9] Y. K. Wu, E. Forest and D. S. Robin, Phys. Rev. E 68, 046502 (2003).
[10] M. Borland, "User's manual for elegant, version 25.0.2" (2012).
[11] H. S. Dumas and J. Lasker, Phys. Rev. Lett. 70, 2975 (1993).




ISBN 978-3-95450-115-1